doi:10.1017/S1431927617009679
Microsc. Microanal. 23 (Suppl 1), 2017

Characterization of MEL defects in 2 – Dimensional MFI nanosheets

Prashant Kumar,[1] Han Zhang,[1] Neel Rangnekar[1], Michael Tsapatsis,[1] K. Andre Mkhoyan[1]

[1]Department of Chemical Engineering & Materials Science, University of Minnesota, Minneapolis, MN 55455.

MFI-type zeolite is a microporous silicon-oxygen framework that has been important for several decades due to its o-/p-xylene separation properties in petroleum industry. In 1980s, significant TEM characterization work was done on large-sized MFI-type zeolite crystals, leading to imaging and electron-diffraction studies of its crystal structure, identification of defects and detection of MEL intergrowth within the MFI framework [1-2]. Since then, development of novel synthesis techniques has enabled the creation of 2-dimensional MFI nanosheets [3-4], while development of aberration corrected TEM has pushed the resolution limit of electron microscopes. Capitalizing on these scientific advancements, we revisit the problem of MEL intergrowth within MFI framework by characterizing this defect at the atomic scale in 2-dimensional nanosheets using aberration corrected TEM.

Electron-diffraction and BF-TEM data was collected on [010] oriented MFI zeolite nanosheets using FEI Tecnai G2 F30 (S)TEM equipped with TWIN pole piece (C_s=2 mm) and a Schottky field emission electron gun operating at 300 kV. HAADF-STEM imaging was performed on aberration corrected FEI Titan 60-300 (S)TEM, equipped with FEI SuperX EDX detector, operating at 200 kV.

Analysis of experimental data was performed by developing new image processing algorithm constituting radial weiner filtering and cross-correlation to identify the MFI and MEL unit cell in BF-TEM and HAADF-STEM mode (Figure 1a-c). These unit cell images were used as templates in a matching algorithm developed to obtain the spatial distribution of MEL within MFI framework (Figure 1d). Analysis of electron diffraction data was performed by 2D-gaussian fitting of (102) diffraction spot from experiment, which showed streaking in a*-direction (Figure 2). Comparison of fitting data with *Multislice* simulations [5] of electron diffraction patterns and structure factor calculations allowed us to compute the average MFI domain size and MEL content within the 2D zeolite nanosheets. In this study, we observed the prevalence of MEL-type defect in a targeted synthetic route for MFI-type framework suggesting a dynamic growth process, which requires precise control and further understanding of chemical synthesis [6].

References:

[1] J. M. Thomas *et al*, Chem. commun.**, 24,** (1982), 1380-1383.
[2] G. R. Millward *et al*, Faraday Trans 2 **79,** (1983), 1075-1082.
[3] M. Choi *et al*, Nature **461**, (2009), 246-249.
[4] K. Varoon *et al*, Science **334,** (2011), 72-75.
[5] E. J. Kirkland, "Advanced Computing in Electron Microscopy", ed. 2, (Springer, New York), 2010.
[6] This work was supported as part of the Catalysis Center for Energy Innovation, an Energy Frontier Research Center funded by the U.S. Department of Energy, Office of Science, Basic Energy Sciences under Award DE-SC0001004.

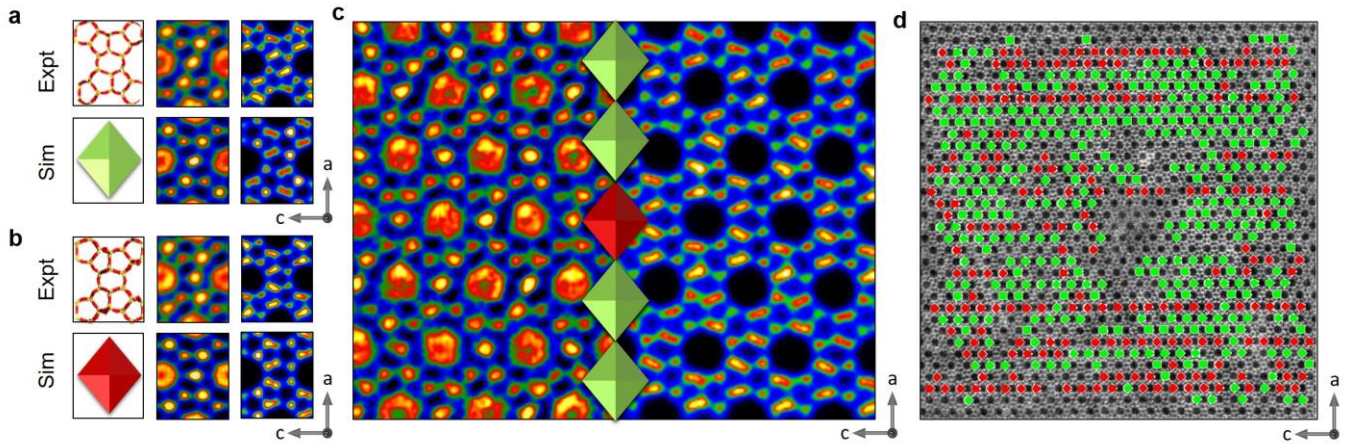

Figure 1. Unit cell of **a,** MFI and **b,** MEL oriented along b-axis is imaged in BF-TEM mode, HAADF-STEM mode and compared with simulated images, respectively. **c,** Cross-correlated BF-TEM and HAADF-STEM image showing a unit cell of MEL inserted between two MFI unit cells. **d,** HAADF-STEM image of a faulted nanosheet overlaid with templates of MFI (green) and MEL (red) as shown in a and b respectively, detected using template matching algorithm in MATLAB.

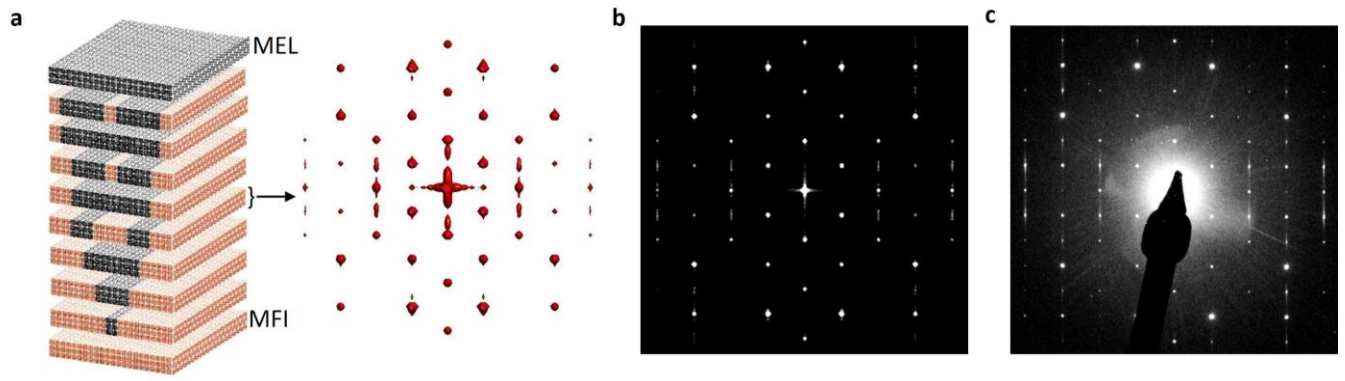

Figure 2. a, Atomic structure models of MFI/MEL intergrown nanosheets, with the corresponding structure factor simulation in MATLAB for one structure model. **b,** Multislice simulation of the diffraction pattern for a nanosheet model highlighted in a. **c,** Experimentally observed diffraction pattern of a nanosheet oriented along [010] zone axis, which matches closely with the structure factor and Multislice simulation shown in a and b, respectively.

https://doi.org/10.1017/S1431927617009679 Published online by Cambridge University Press